Dolgion Erdenebat (Lead author)[1]
dolgion.erdenebat@uni.lu
Danièle Waldmann (Co-author 1, corresponding author)[1]
daniele.waldmann@uni.lu
[1] University of Luxembourg, Institute for Civil Engineering and Environment, 6, Avenue de la Fonte, L-4364 Esch-sur Alzette, Luxembourg,

Application of the DAD method for damage localisation on an existing bridge structure using close-range UAV photogrammetry

ABSTRACT: A novel damage detection and localisation method, the so-called Deformation Area Difference method for localisation of damages in bridge structures is introduced. The method is based on static load-deflection experiments with the prerequisite of high precise deflection measurement. This study presents the first experiences of applying the DAD method on a real bridge structure. The investigated structure is a prestressed concrete slab bridge with a span of about 27 m, which was built in 2013. The loading on the bridge is applied using six heavy trucks, each weighing up to 32 t. A wide range of the modern measurement technologies were used to achieve high precision measurements of the bridge deflection along the longitudinal axis, namely the photogrammetry using a big size drone, laser scanner, total station, levelling and displacement sensors. The performed load-deflection test was non-destructive since the maximum deformation did not exceed the serviceability limit state. The exercise of the novel damage detection and localisation method on a real structure initiated further optimisation opportunities of the DAD method and the study of its limits. Several boundary conditions and methodical influence factors related to the applicability of the proposed method were analysed, such as impacts of measurement precision, damage degree, the position of damage, and the number of measurement repetitions.

1. Introduction

There exists an enormous amount of bridge structures worldwide guaranteeing a functional infrastructure as part of the public space. However, the constantly rising average age of bridges and the growing weight of heavy transporters further increase the applied stresses on the existing bridge structures [1]. The construction industry mostly uses natural resources. Therefore, the preservation of existing structures has a decisive influence on the ecological balance [2]. In general, the quality of the condition assessment depends on the experience of the bridge inspector and the applied state-of-the-art inspection methods. Although technological innovation has become much more prevalent in many areas, the construction industry is still

lagging to implement new technologies in their processes [3] and, therefore, the bridge inspection according to the state-of-the-art is still mainly carried out by visual inspection [4].

Generally, the damages of bridge structures can be recognised on the structure surface by visual inspection. However, in case, the damage occurred inside the load-bearing structure, the damage detection becomes highly complex and the loss of stiffness cannot be detected in time. Some bridge inspection methods such as ultrasonic [5] or endoscopy are capable to examine the interior of the structure to a certain extent, but the location of the damage should be identified in advance. Recently, various research projects are dealing with the objective of damage assessment in bridge constructions based on different approaches. Oskoui et al. [6] developed a method for detection of cracks in bridges based on the structural influence line from moving load and the measurement of strains at multiple positions. The method was tested on a five-span 332-meter bridge and the analysis of the results led to the identification of five locations with anomalies. Visual inspection verified mini cracks at two locations and three misaligned sections. The method was mostly influenced by the big noise effect from the strain measurements. A comparative study based on strain gauges and influence line for damage detection in bridge structures was carried out by Wu et al. [7]. The focus of the study is on truck weight variations and vehicle speed to procedure the influence line. The authors report that the damage identification method is not affected by the truck speed but by the weight of the truck. An additional study for the damage extension is done based on a 1:10 scaled bridge model. The authors announced about higher damage identification accuracy for damages greater than 10 %. Further damage detection methods based on influence line are presented in [8] [9] [10] [11]. Based on the theoretical principles, the detection of stiffness changes is feasible using the influence line, but the accuracy of the measurement related to the noise effect significantly affects the result of damage detection [12].

Besides to the examination of the moving load and the analysis of the resulting influence line, the investigation of the static load-deflection experiments on bridge structures provides information about the stiffness changes and the damages [13]. As bridge structures are built to bypass local obstacles, such as river, slope, road and valley etc., not all measurement techniques are applicable and it is often difficult to carry out deflection measurements along a bridge structure [14] [15].

Le et al. [16] present a method for damage localisation based on static load-deflection experiments. This study shows the results from finite element calculations for several steps of damage degrees. The theoretical results without noise effect show successful detection of damages at two positions for a one-span beam. Furthermore, a laboratory test was performed, where the cross-section of a U-profile is reduced at two different positions and the resulting deflection of a loading test is measured at seven locations with displacement transducers. Opposed to the finite element result, the experiment delivers deflection values affected by a measurement noise effect. The clear identification of damage is questioned and further examination with different noise level are examined [17] [18] [19].

Load-deflection tests on bridges have a long history and usually are carried out before the opening of the bridge or after the rehabilitation to demonstrate to the public about its load-bearing capacity. However, innovative measurement techniques open new possibilities to develop novel methods based on existing experiences and knowledge. Such a novel technique is the newly developed Deformation Area Difference (DAD) method for detection and localisation of damages in bridge structures, which is based on high precision deflection measurements of static load-deflection tests. The state-of-the-art methods for damage detection and the DAD method are presented based on theoretical examples and a laboratory experiment in [20]. The laboratory experiment consists of a reinforced concrete beam with the stepwise loading process. The study presented the successful identification of the cracked areas using the DAD method. Further development of the method tested on an additional laboratory experiment is published in [21]. The main development of the method was to find out how to smooth the measurement noise to localise only the damages.

The current research investigates the boundary conditions and the needed measurement accuracy related to the detection of damages using the DAD method and presents the first application of the DAD method on a real prestressed concrete bridge with a span of about 27 m. All impact factors influencing the damage detection sensibility, such as the measurement precision, the degree of the damage, damage position, required amount of experimental deflection, repetition of measurements etc., are investigated. The static load was applied using six heavy trucks, each of them weighing about 32 t (Figure 1). This study starts with the introduction of the theoretical background of the DAD method. Subsequently, the experimental setup of the experiment on the bridge is presented, followed by an investigation of the influencing factors for the DAD method.For the bridge experiment carried out in the current research, various modern measurement techniques were applied such as photogrammetry, laser scanner, total station, levelling and displacement sensors. Levelling delivered very high precision and was easy handling for application on a bridge structure. In particular, the application of photogrammetry installed on a big size drone showed very promising results and suitable application. Finally, an analysis is carried out to evaluate the detection of the degree of damage depending on the measurement precision, deflection size, damage position and measurement repetition.

Figure 1. Loading of the bridge by six trucks

2. Deformation Area Difference (DAD) method

The DAD method is developed to detect local damages in bridge structures. It takes into account the measured deflection of the structure $w_d(x)$ and the deflection from a reference system $w_t(x)$ (Figure 2). Beside an initial deflection measurement, also a simplified linear finite element model of the investigated bridge structure can be applied as a reference system. However, it is important that the reference system has a continuous deformation curve and it should consider the stiffness influencing structural parts like cross members, coves, coupling points of the prestressing cables etc. (Figure 2). The density of the values from the reference model should correspond to the density of the measurement points installed on the bridge structure. The DAD method is based on the fact that the measured deflection curve includes information about the local stiffness changes what will be further explained in the following section.

2.1. Relationship between the deflection curve and the stiffness of the structure

The study aims to develop a method to identify stiffness changes influenced by damages. Several research projects worked with the same goal based on dynamic [22] [23] [24] and static responses [25] [26] [27] of bridge structures. Both structural responses are influenced by stiffness changes e.g. due to damage. The localisation of the damage based on dynamic analysis presents more difficulties because the structural response on a dynamic excitation such as natural frequencies, mode shapes or damping are based on a global behaviour of a structure which renders the identification of local effects difficult. In contrast, the static structural responses deliver very promising results [28] [29].

The DAD method allows the localisation of stiffness reducing damages based on the deflection measurement of bridge structures. The stiffness of a structure under loading can be analytically calculated from the multiple derivatives of the deflection curve. The first derivative of the deflection corresponds to the inclination angle (equation (1)).

$$w'(x) = \frac{\delta w(x)}{\delta(x)} = \varphi(x) \tag{1}$$

In case of small deflections, the second derivative of the deflection curve, respectively, the first derivation of the inclination angle corresponds to the curvature of the structure (equation (2)). This condition is fulfilled when non-destructive load-deflection experiments are performed within the serviceability limit state. The determined curvature of the structure k(x) can be expressed as the ratio between the bending moment M(x) and the stiffness EI(x) (equation (3)). The known parameters of equation (3) are the curvature as the second derivative of the deflection curve and the bending moment resulting from the experimental load. Thus, each change of the stiffness EI(x) should be identifiable using the curvature and the bending moment. However, there are some issues related to the direct use equation (3) for identification of damage.

$$w''^{(x)} = \varphi'(x) \cong k(x) \tag{2}$$

$$k(x) = \frac{M(x)}{EI(x)} \tag{3}$$

Opposed to the theoretical models, the real measurement of the deflection include measurement noise, which depends on the precision of the applied technique. Furthermore, the noise effect included in the deflection curve is increased by multiple derivations (equation (2)). The stiffness values expressed in equation (3) comprise the information about damage, planned stiffness changing areas (Figure 2) etc. Therefore, the challenge is to distinguish the discontinuities in the curvature curve between damage, measurement noise effect and stiffness changes inherent in the cross-section configuration. At this point, the DAD method becomes effective as it provides an alternative possibility to identify damages without using multiple derivations. It also takes into account the measurement noise effect and the stiffness changes resulting from the shape of the structure.

2.2. Background of the DAD-method

The DAD method investigates the difference in the area (green area in Figure 2) between the theoretical curves of the deflection line, the inclination angle and mainly the curvature with their corresponding curves

from the experimental measurements. The deflection curve from the theoretical model of the bridge structure ($w_t(x)$ black curve in Figure 2) considers all planned stiffness influencing parameters of the structure such as cove, cross member etc. The principle of the DAD method is presented using a theoretical bridge girder with local damage of 60 %. The high amount of damage degree is chosen to clearly display the discontinuity resulting from the damage effect in the curvature curve. As long as the damage is not exactly at the point of a planned stiffness change, even the smallest degree of damage can be detected based on theoretical values. However, the real deflection measurement is affected by measurement noise which influences the detectable degree of the damage. Further investigation about the detectable degree of damage is presented in Section 5.2.

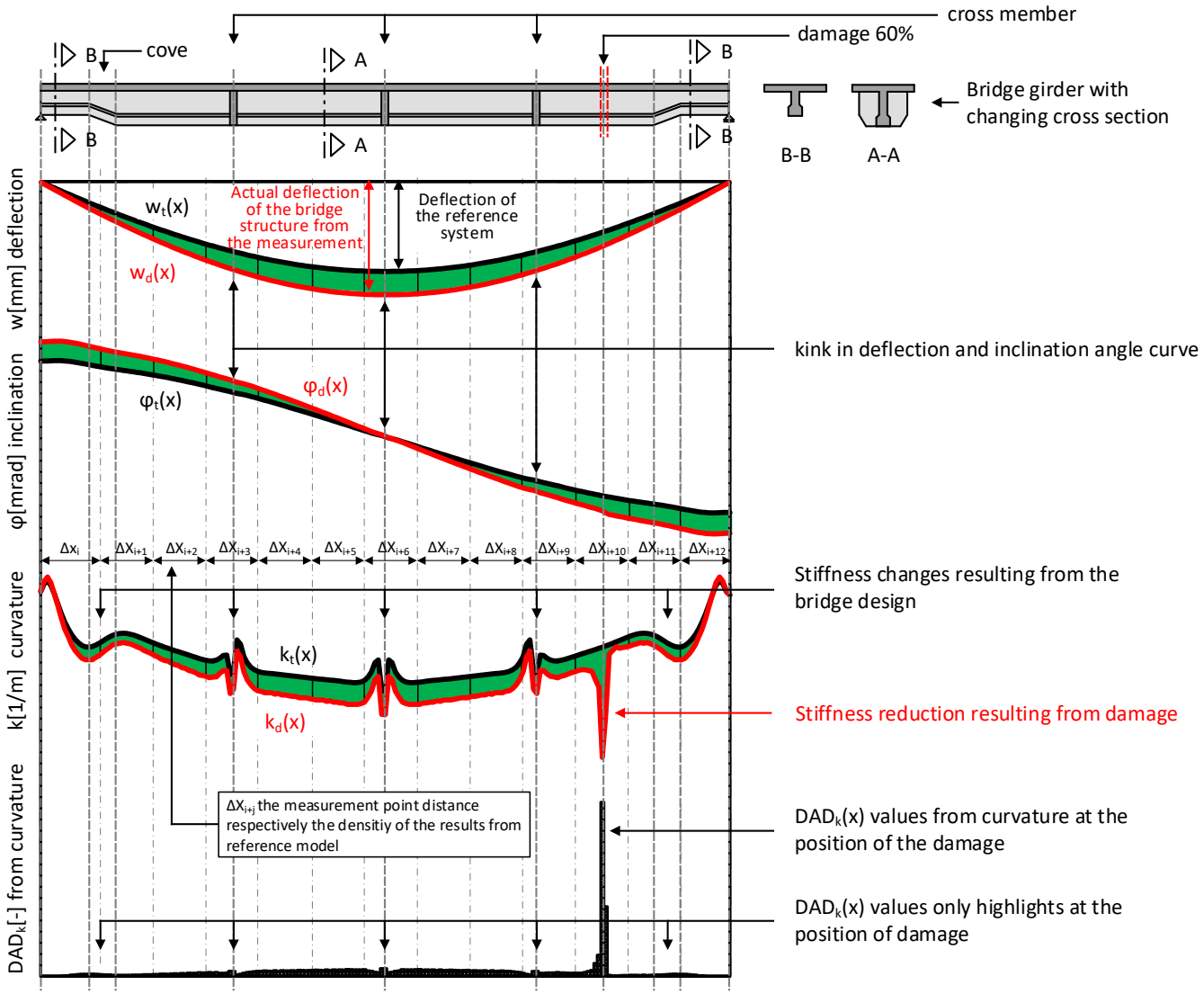

Figure 2. Principle of the Deformation Area Difference (DAD) method

$w_t(x)$ Deflection of the reference system (theoretical model)

$w_d(x)$ Actual deflection of the bridge structure from the measurement

$\phi_t(x)$	Theoretical inclination angle from the reference system
$\phi_d(x)$	Inclination angle from the first derivation of the measured deflection
$k_t(x)$	Reference curvature from the theoretical model
$k_d(x)$	Curvature from the second derivation of the measured deflection
Δx_i	Distance between measurement points (mesh size of the model)
green area	Area between the reference system and the measurement
$DAD_k(x)$	Deformation Area Difference (DAD) value from curvature
$A_{k,d,i}$	Area section under the damaged curvature curve
$A_{k,t,i}$	Area section under the reference respectively undamaged curvature curve
$\Delta A_{k,i}$	Area difference between damaged and undamaged curvature curve

Once the theoretical and experimental curvature curves are determined, the area under both curves from reference system and measurement is computed using the integral of the curvature functions (equations (4) and (5)), and the area difference is calculated according to the equation (6).

$$A_{\kappa,d,i} = \int_{i-1}^{i} \kappa_{d,i}(x)dx \tag{4}$$

$$A_{\kappa,t,i} = \int_{i-1}^{i} \kappa_{t,i}(x)dx \tag{5}$$

The disintegration of the function of curvature k(x) leads back to the function of the inclination angles φ(x) because the derivation of the inclination angle corresponds to the curvature (equation (2)). In other words, the DAD values for the curvature can be directly calculated using the first derivation of the deflection values respectively using the inclination angle values (equation (6)). Using this method, the multiple derivations and the step of approximation according to equation (2) is avoided.

$$\begin{aligned}\Delta A_{k,i} &= \int_{i-1}^{i} \kappa_{d,i}(x)dx - \int_{i-1}^{i} \kappa_{t,i}(x)dx = \\ &= [\varphi_d(x)]_{i-1}^{i} - [\varphi_t(x)]_{i-1}^{i} = \varphi_d(x_i) - \varphi_d(x_{i-1}) - \varphi_t(x_i) + \varphi_t(x_{i-1})\end{aligned} \tag{6}$$

The DAD method subdivides the area differences into several small sections Δx_i, as shown in Figure 2. The length of the section depends on the density of the measurement points and the mesh size of the finite

element model used as a theoretical reference. Then, each difference area is separately squared and divided by the sum of the squared areas according to equation (7) to filter out of the known stiffness changing areas from the reference model and to represent the damaged section in a squared scale. Due to this normalisation, the effect of damage is strongly highlighted, which allows the increase of the sensibility of the method on damage detection.

$$DAD_{\kappa,i} = \frac{\Delta A_{\kappa,i}^2}{\sum_{i=1}^{n} \Delta A_{\kappa,i}^2} = \frac{[\varphi_d(x_i) - \varphi_d(x_{i-1}) - \varphi_t(x_i) + \varphi_t(x_{i-1})]^2}{\sum_{i=1}^{n} [\varphi_d(x_i) - \varphi_d(x_{i-1}) - \varphi_t(x_i) + \varphi_t(x_{i-1})]^2} \quad (7)$$

2.3. Smoothing of the measurement noise

In case the measurement precision is known, the effect of noise can be filtered out from the measured deflection line. This procedure allows the reliable localisation of stiffness changes out of the range of the measurement noise. A detailed case study with a theoretical example and a laboratory test is presented in [21] and summarized in the following. The essential background of the noise smoothing process within the measurement standard deviation is applied based on equations (8) and (9). First of all, a polynomial regression $w_r(x)$ is determined based on the deflection curve $w_d(x)$, which is affected by noise (equation (8)). Then, the raw deflection curve $w_d(x)$ is filtered within the measurement standard deviation s(x) and the smoothed deflection curve $w_{d,s}(x)$ can be obtained using equation (9).

$$\Rightarrow w_r(x) = \sum_{i=1}^{n} a_i x^i \quad (8)$$

$$\begin{cases} w_{d,s}(x) = w_d(x) - 0{,}50 \cdot s(x) \geq w_r(x), & if \quad w_d(x) \geq w_r(x) \\ w_{d,s}(x) = w_d(x) + 0{,}50 \cdot s(x) \leq w_r(x), & if \quad w_d(x) < w_r(x) \end{cases} \quad (9)$$

With:

$w_r(x)$	Polynomial regression
$w_d(x)$	Actual deflection of the bridge structure from the measurement
$w_{d,s}(x)$	The deflection function of the bridge structure from the measurement after smoothing
s(x)	Standard deviation resulting from the measurement technique

2.4. Identification of damages (outliers)

The DAD method is supposed to highlight the discontinuities resulting from a local damage. However, the evaluation is affected by the measurement noise and all stiffness influencing parts of the structure (Figure 2). After the application of the smoothing process, the outliers from the DAD values highlight the position of damages. However, it remains challenging to differentiate whether the highlighted discontinuities result

from damage, from the measurement noise effects or from a stiffness change in the structure. Therefore, the widely used box plot method [30] [31] is applied to identify the real outliers of the DAD values (Figure 3).

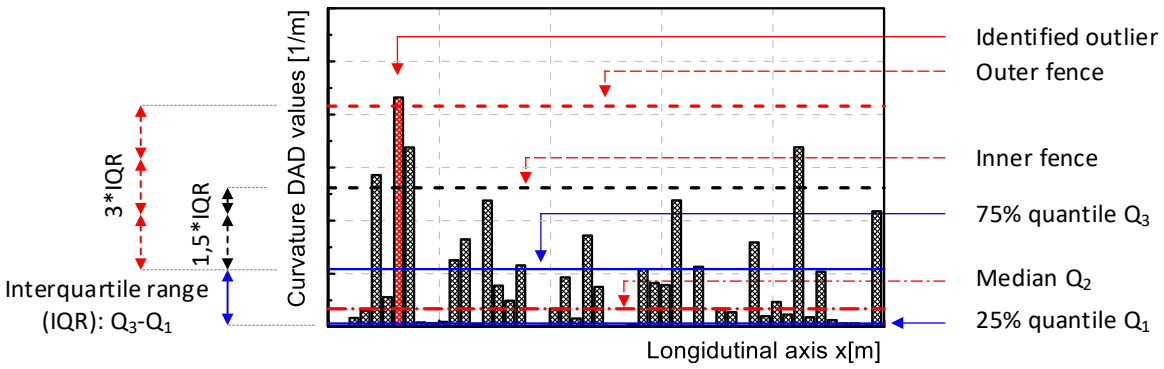

Figure 3. Identification of outliers based on the box plot method

The application of the box plot method defines an inner boundary value and an outer boundary value. The values from the investigated data which fall over the inner boundary value are considered as a minor outlier and those values over the upper boundary value are considered as major outliers. In a first step, the lower 25% quantile value (Q1 in Figure 3) and the upper 75% quantile value (Q3 in Figure 3) are computed to determine the interquartile range (IQR in Figure 3). Then, the inner boundary value is defined as the 75% quantile value plus 1.5 times the IQR, and the outer boundary value is defined as the 75% quantile value plus 3 times the IQR. The identified DAD values as a major outlier area are considered as locations where damage can be observed (Figure 3).

In the case of small damages in bridge structures, the discontinuity from the DAD values does not clearly highlight. Therefore, the identification of outliers enables the differentiation between the actual outlier and the discontinuity resulting from the noise effect. If outliers have been found, the DAD method was not able to identify any damages within the measurement precision. The impact of the damage position and the measurement precision on the detectable degree of damage is discussed in sections 5, 6 and 7.

3. Description of the bridge

The applicability of the DAD-method on a real bridge structure is investigated on a road bridge in Altrier, Luxembourg. The bridge was built in 2013 and serves as an overpass bridge crossing over a traffic road. The structural bridge superstructure is made of prestressed concrete with a span of about 27 m (Figure 4). The height of the bridge cross-section amounts to 93 cm. In total, the prestressing consist of thirty-six parabolic post-tensioned tendons with nineteen strands of class 1860 MPa. Concrete of compressive strength class C45/55 according to EC2 [32] was used. According to the official static design documents,

the bridge is designed to accommodate trucks with a maximum weight limit of 60 tons. The cardinal direction of the bridge is oriented from the southwest (Luxembourg City) to northeast (Echternach), which allowed a uniform, natural illumination of the bridge side from morning until the afternoon. The favourable lighting of the structure was an optimal condition for the application of photogrammetry.

Figure 4. The experimental bridge in Altrier in Luxembourg

3.1. Applied techniques

The high precision measurement of the deflection line along the longitudinal axis of the bridge is an essential prerequisite for the successful application of the DAD method. On the one hand, the closer the distance between the measuring points, the higher the achievable precision on the localisation of the damage. However, on the other hand, a higher density of the measuring points leads to shorter height differences between the measuring points, which means that higher measuring accuracy is required to observe any differences. Therefore, it is important to find an optimum between these conditions. The different measurement techniques, which were applied for the experimental test, are as follows:

- Laser scanning: A laser scanner of type Leica P20 was used. This measuring unit can scan one million of measuring points per second to generate a point cloud with 0.8 mm density and has a range of up to 120 m [33].
- Total station: Two total stations of type Leica TS30 and Leica TS60 with very high accuracies, particularly in angle measurement (0.15 mgon) were applied [34]. Therefore, both total stations have been positioned at two different locations, and the targets have been measured using the angular intersection.
- Levelling: The levelling unit of type Leica DNA 03 with very high precision in height observations was used. The precision of the electronic measurement with the help of invar staff amounts to 0.30 mm [35]. The digital invar staff enables the faultless and precise recording of the measurement values.

- Photogrammetry: The technical equipment used for photogrammetry is a full-frame camera Nikon D800 set on a tripod and a medium-format camera Fujifilm GFX50S installed on a big size drone DJI Matrice 600 as shown in Figure 5. The calibration of both cameras was performed using the test-field calibration method. The captured images were processed using the software Elcovision 10 [36].
- Displacement sensors: Two displacement sensors from HBM [37] with the length of 50 mm have been applied among other things to enable the real-time monitoring

In addition, several temperature and humidity sensors were installed above and under the bridge to monitor the environmental conditions. Furthermore, an infrared camera of type InfraTec Variocam was used to observe the temperature distribution on the surface of the bridge. The photogrammetry with Nikon D800 is set using a tripod from a distance of about 10.0 m and 15.0 m from the bridge. The pictures are captured at every 2.0 m along the longitudinal axis of the bridge. The second measurement with photogrammetry is carried out using a Fujifilm GFX50S on a drone. The flight with the drone took place fully automatically, and the camera GFX50S took pictures every 2 seconds. The flights are done in two different heights, namely one at the same height as the bridge deck and one at about 2.5 m from the ground. The distance of the drone to the bridge amounts to about 12.0 m.

Figure 5. The drone DJI Matrice 600 and the camera Fujifilm GFX50S hold by a gimbal

3.2. Experimental setup

The experimental setup installed on the southeast side of the bridge is schematically shown in Figure 6. Fifty-one photogrammetry targets were mounted below the cross-section of the bridge structure at a distance of 50 cm to each other, and each ten reference targets were positioned at both bridge abutments. The measurement with levelling is carried out on the top of the bridge with 3.0 m distances. The

measurement with the laser scanner is done from a single position orthogonal to the centre of the bridge at 15 m from the bridge.

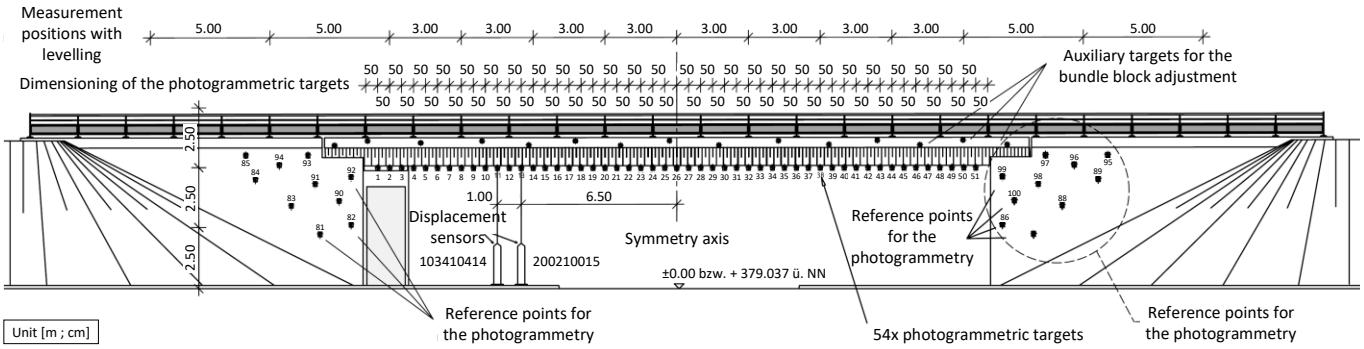

Figure 6. Side view of the experimental setup

Part A of Figure 7 shows the installation process of the photogrammetry targets and part B the dimensions of the setup. The used photogrammetric targets [36] have been printed out on dull adhesive films which are usually used for automobile foliation. The dull films have the advantage for the capturing process that it is not reflected by the sun. The adhesive films are resistant to ultraviolet light and rain or water.

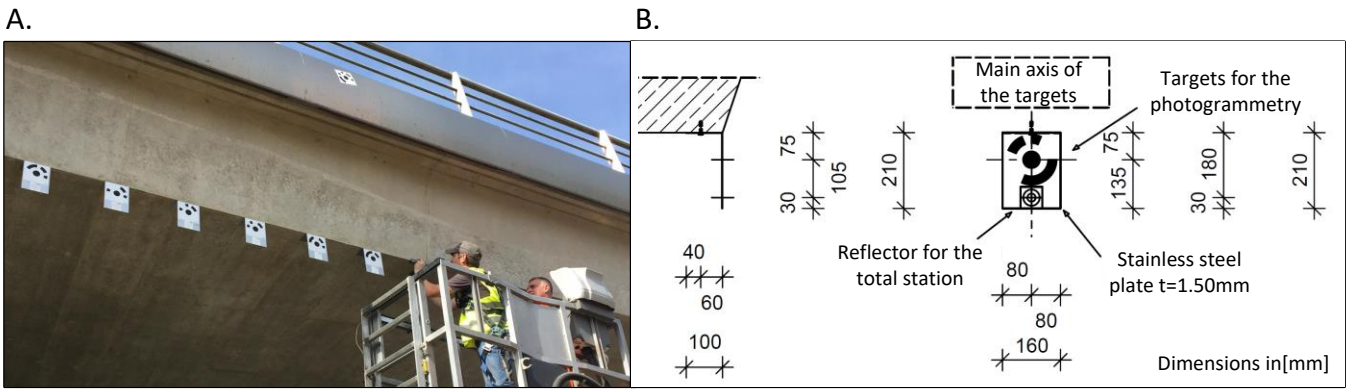

Figure 7. A installation of the targets; B. Dimensions of the setup for targets

For the measurement with the total station, the same targets as for photogrammetry were used. Both displacement sensors have been installed at 6.5 m respectively at 7.0 m from the centre of the bridge, as shown in Figure 6. In addition, the deflection of the bridge was measured with two displacement sensors. The height of the bridge cross-section amounts to 93 cm and at the mid to 1.075 m (Figure 8). Since a large number of measurement techniques were applied during the experiment, the whole traffic was closed from nine in the morning to four in the afternoon for totally seven hours.

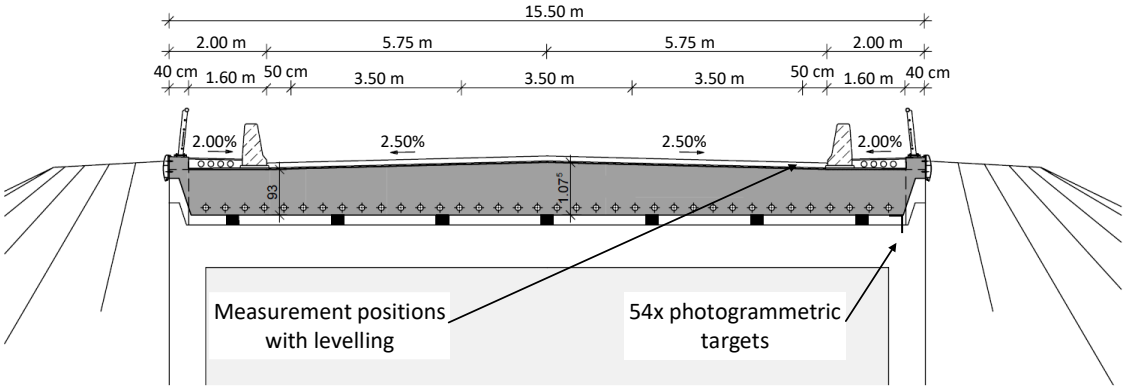

Figure 8. Cross-section of the bridge

3.3. Finite element model of the bridge

A finite element model of the bridge was designed using the software Sofistik (Figure 9). The FE-model functions as a reference system for the application of DAD-method. Furthermore, the dimension of the experimental load and the amount of the required trucks was defined based on the FE-calculation and the existing static documents of the bridge. The FE model is carried out based on linear calculation, which corresponds to the non-destructive load-deflection experiment on the bridge within the serviceability limit state. The realistic modelling of the bridge structure is usually a major challenge. The model updating is often required based on dynamic or static experimental results to enable the increase in the accuracy of the FE model. As already mentioned, the DAD method requires a theoretical reference system of the investigating bridge structure. However, the model does not have to respect a high requirement regarding the accuracy of the FE model. In other words, the following conditions are important for the creation of the reference system:

- Static system respectively the span lengths
- Consideration of the changes in cross-section or changes in local stiffness changes
- Position of the experimental load

In return, the following points are not needed to be represented according to the real conditions of the studied structure, which makes the modelling of the reference system much easier:

- Amount of the structural deflection
- Amount of the load
- Global effects from both the dead load and the temperature
- Spring stiffness of the support structure
- Deflection due to shear force

- Effects from creep and shrinkage
- Linear material properties and linear calculation

The DAD method considers the area between the measured curvature curve and the reference curvature curve. The considered area is divided into several sections, which enables a relative comparison, respectively only identifies local changes in the deflection behaviour of the structure.

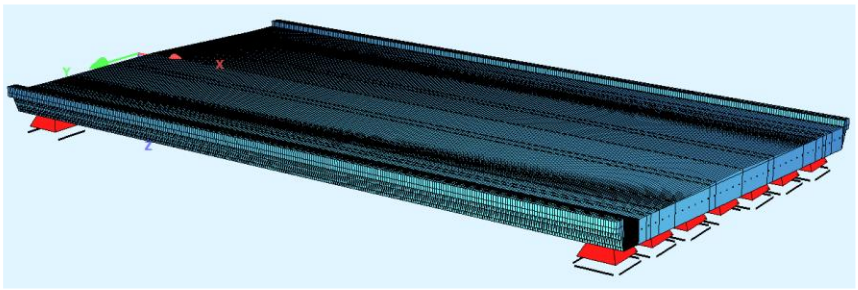

Figure 9. Finite element model of the experimental bridge using the software Sofistik

3.4. Loading of the bridge

The DAD method for localisation of damages bases on the measurement of the deflection curve of a bridge structure. The easiest way to apply loading on a bridge structure is to use heavy trucks. However, on the one hand, the load should not exceed the serviceability-limit-state, and on the other hand, the amount of deflection should be as big as possible to generate a measurable bridge deflection. The required amount of experimental deflection is investigated in section 5.3.

Within the presented bridge experiment, respecting the two constraints described in the previous paragraph, the determination of the loading led to six heavy trucks with a weight between 31 t and 33 t per truck (Figure 1 and Figure 10). During the experiment, the bridge structure is loaded step by step and the structural deflection is monitored in real-time using both displacement sensors (Figure 6).

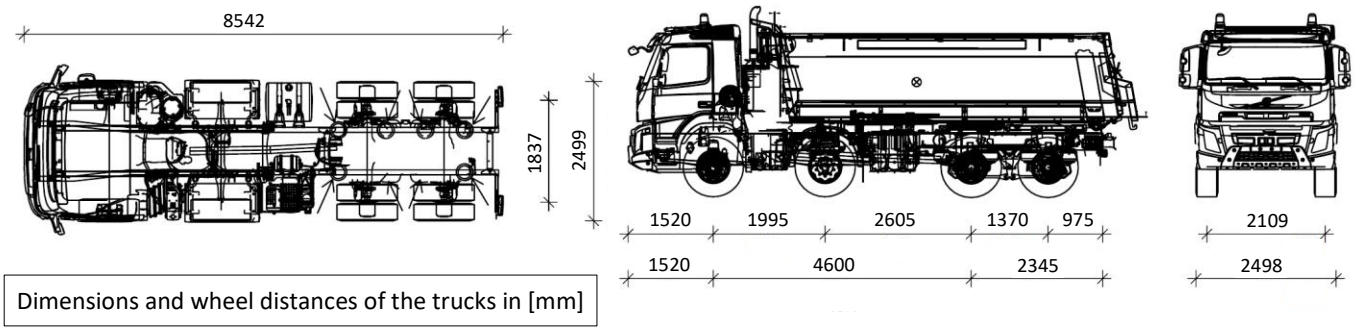

Figure 10. Dimensions and wheel distances of the trucks [38]

Figure 11 shows the expected and measured deflection as a function of time and related to the consecutive loading of the bridge by the six trucks. The presented deflection values (vertical axis) as a function of time (horizontal axis) were measured by both displacement sensors (Figure 6). The values in brackets represent the expected deflections resulting from the FE calculation. For trucks number 1, 3 and 5, small peaks can be observed at the beginning of the deflection curves due to the crossing of the bridge centre by the trucks before reaching their final position. The measured deflection values always lay below the expected values from FE calculation, which allowed to increase the number of trucks to all planned six trucks. The maximum deflection of the bridge at the midpoint amounted to about 11.0 mm, which corresponds to a span deflection ratio of about L/w = 27.0/0.011 ≈ 2500.

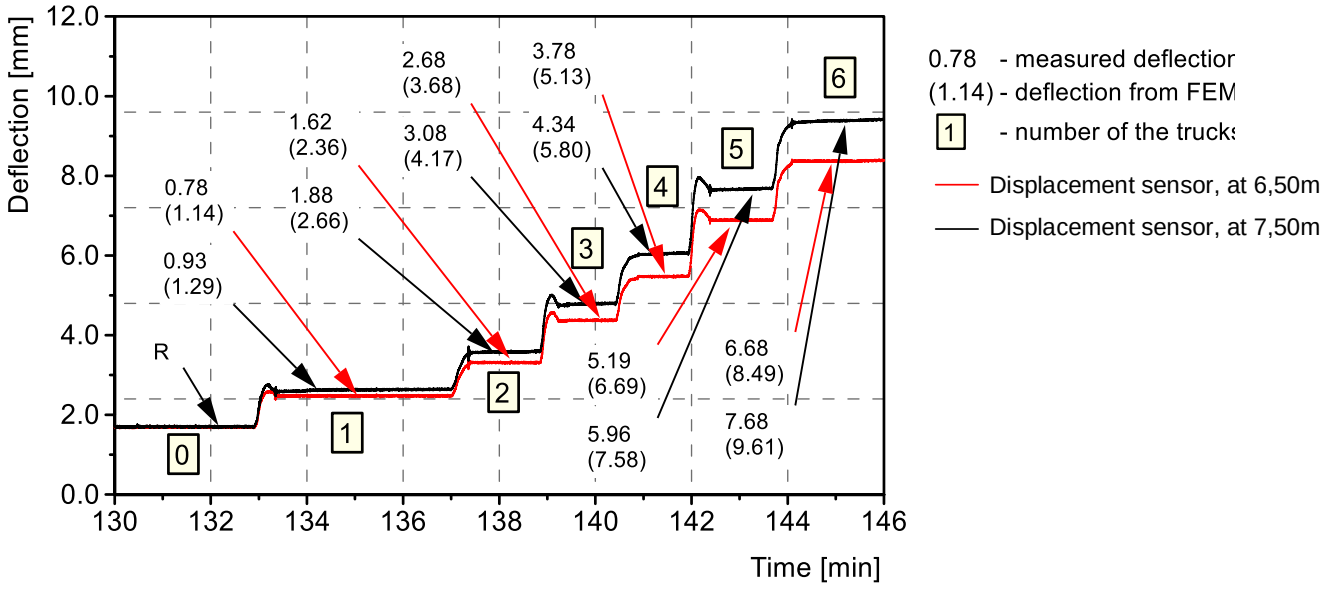

Figure 11. Loading of the bridge and measurement of the deflection by displacement sensors

3.5. Environmental conditions during the test

Figure 12 summarises the temperature and humidity measurements over time on top and under the bridge, as well as the deflections measured by the displacement sensors. The sensors are installed at about 8:40 am, which is visible in the diagram. After about 20 minutes, the sensors have been adapted to the surrounding conditions. The humidity and temperature sensors are battery operated and were switched on the day before the test and switched off the next day after the experiment. Therefore, Figure 12 includes recorded data about the humidity and temperature before and after the test day. These data show the environmental conditions of the transport vehicle and have no significance for the test conditions. The air humidity

amounted to about 85% and decreased over time. The temperature slowly increased during the test day and amounted on average to about 16°C. The sky on the experimental day was cloudy, which represents an optimum condition for the use of the photogrammetry technique.

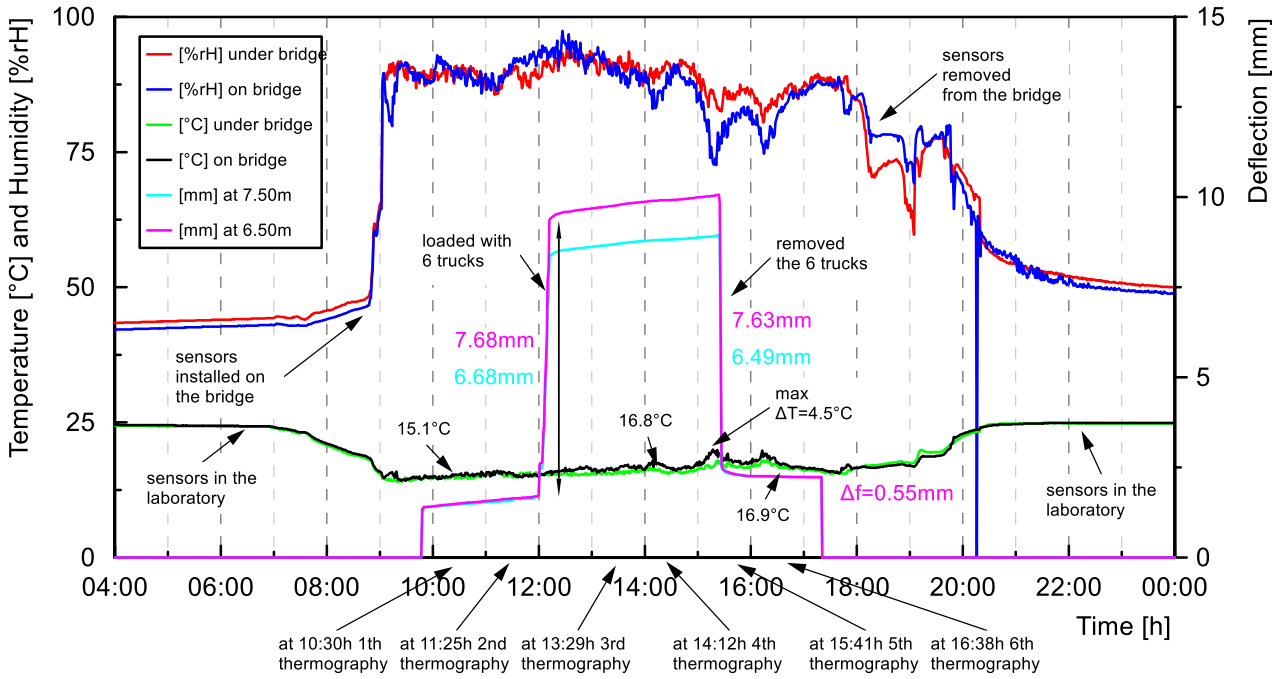

Figure 12. Determined humidity and temperature of the bridge Altrier, as well as its deflection measured by the displacement sensors on the test day

Figure 13 shows the six thermography images of the bridge, which were captured at an hourly basis from the start to the end of the experiment. Until 14:12h, uniform temperature distribution at the surface of the bridge can be observed, which were ideal conditions for the experiment and mainly resulted from the cloudy weather conditions. In contrast, the highest surface temperature difference was recorded at 15:41h, however, only a maximum temperature difference of 1.30°C was observed between the surface in the shadowed area and the areas exposed to the sunlight. Therefore, it can be assumed that the load-bearing structure had an uniform temperature distribution over the whole duration of the experiment. Nonetheless, it should be noted that the application of the DAD method is not affected by a uniform respectively a global temperature change [20]. The temperature change usually affects the whole structure, not at a local position. Since the DAD method carries a relative investigation comparing measured data to a reference data set for the detection of damage, the temperature effect has no influence (see section 3.3).

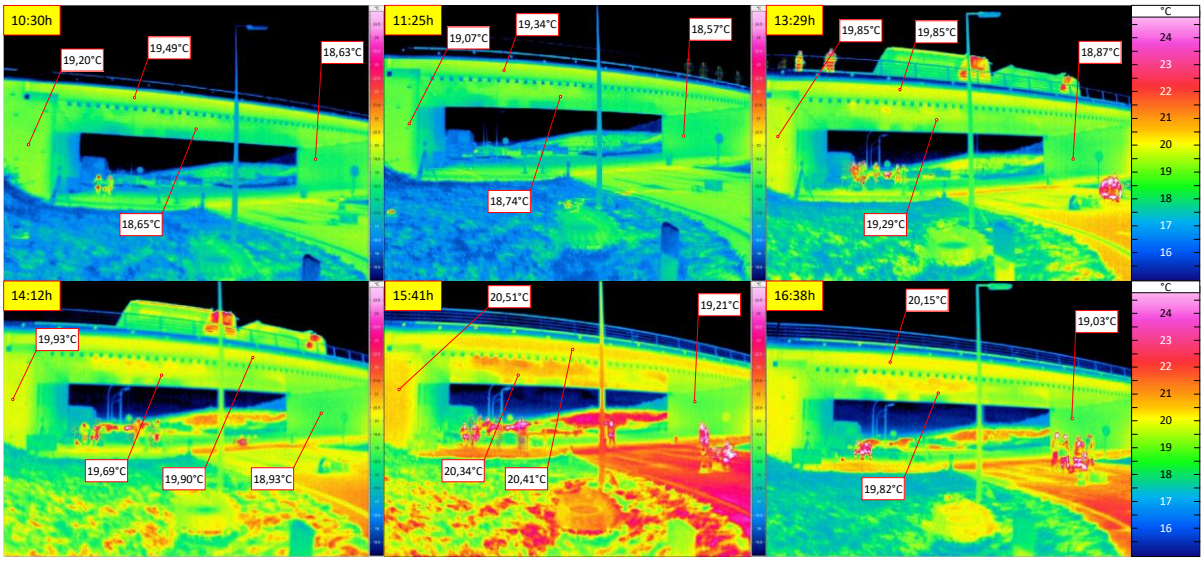

Figure 13. Thermography measurement of the bridge at different periods of the day

4. Results of the bridge experiment

In the past, the DAD method was applied for several case studies based on finite element calculations and on some laboratory experiments [20] [21] [39] [40] [41]. The current study shows the first time the application of the DAD method on a real bridge structure. The major aim for this study was to identify the measurement precision which is able to be achieved on a real-scale structure under outside environmental conditions and not the DAD values themselves as the newly constructed bridge was expected to be without any damage.

4.1. Measurement precisions

In this study, the deflection of the bridge is recorded by several most modern measurement techniques. Part A in Figure 14 shows the deflection of the bridge measured by photogrammetry. The maximum deflection by six heavy trucks amounts to about 11 mm. The targets were placed at a spacing of 50 cm along the longitudinal axis (Figure 14). Applying the photogrammetry, each measuring targets is captured several times from different angles and positions. The photogrammetry measurement was carried out based on the bundle block adjustment of all pictures and, the coordinates of the targets have been determined. The diagram presented in Figure 14 shows the standard deviation of each target with an average value of about 0.07 mm (Part B. in Figure 14).

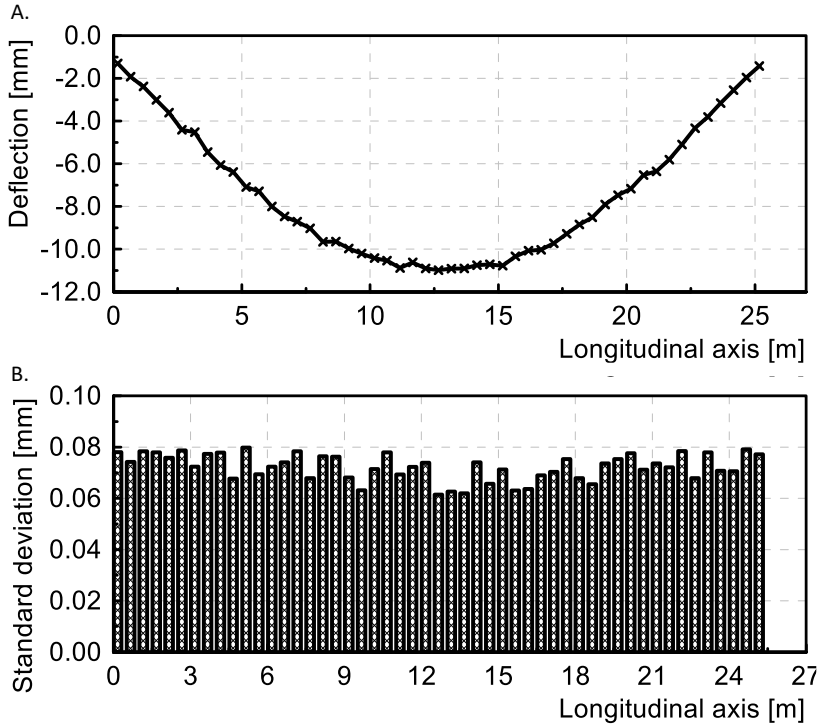

Figure 14. The deflection measurement by photogrammetry using the camera GFX50S and the drone (Part A.) as well as the standard deviation for each target (Part B.)

The precision of the measurement is determined based on the noise effect (Figure 15). The noise from the deflection effect is shown in black, and the measurement noise after the smoothing process according to section 2.3 is shown in red dashed line.

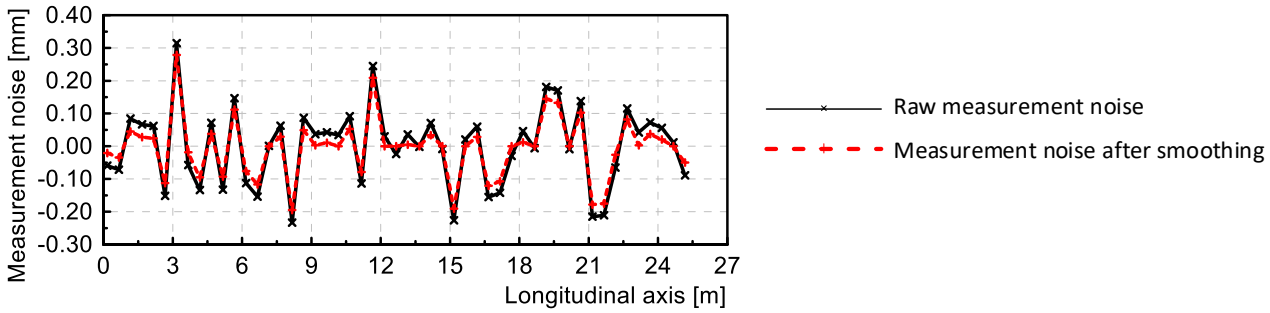

Figure 15. The filtered noise effect from raw measurement and after smoothing

In order to identify the accuracy of the measurement techniques, an exactly calibrated comparative measurement is normally carried out. Within the experiment, several most modern high–precision measurement techniques have been applied. However, every measurement technique delivers normally distributed measurement results. Therefore, in order to determine the standard normal distribution of the measurement results, the measurement noise effect has to be filtered out from the deflection line. Figure 16 shows the determination of the standard deviation of a measurement noise related to a straight line. However, in the case of a deflection measurement (Figure 17), the standard deviation cannot be determined

directly, as shown in Figure 16. A polynomial regression is therefore created from the measurement data, which corresponds to the deflection curve of the experimental bridge structure and is substracted from the measured deflection line. Then, only the noise of the measurement results would remain as shown in Figure 16. The advantage of this procedure is that the precision of the measuring techniques can be compared to each other (Figure 19). The disadvantage is that the polynomial regression does not correspond 100 % exactly to the deflection line and falsifies the result to a small extent. Based on this, the precision of all applied measuring techniques are finally compared by their standard deviations (Figure 19).

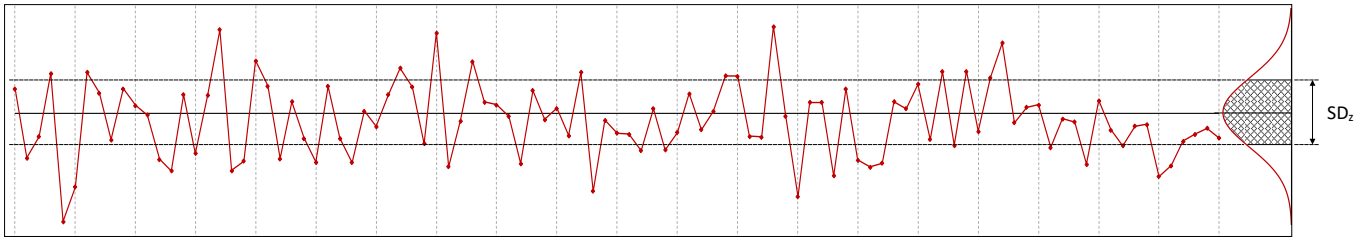

Figure 16. Measurement noise along a reference line and the standard deviation

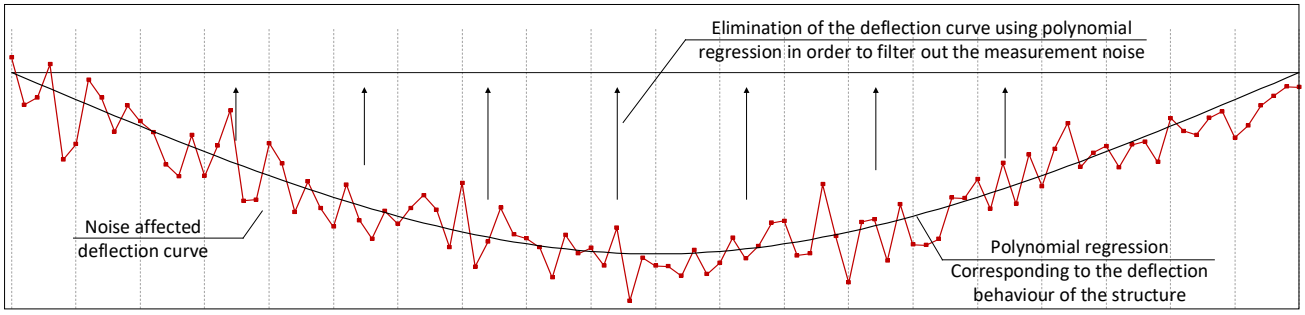

Figure 17. Exemplary, a noise affected deflection line and filtering out the measurement noise using polynomial function

The precision value of 3.0 mm for laser scanning is only an estimated value as the precision of the laser scanner depends on the roughness of the bridge surface, on atmospheric conditions, on internal safety mechanism and measuring configuration. Comparable studies [42] report the accuracies of about 0.50 mm to 5.00 mm for laser scanner Leica P20. Therefore, it is quite possible that the actual accuracy is much better than the estimated value of 3.00 mm. The displacement sensors deliver very high precise deflection values with a standard deviation of 0.0329 mm. However, the application of the DAD method using displacement sensors would not be practical, because of the high number of the required measurement points. The levelling is also a high precision measurement technique, however the precision could be influenced by human handling. The measurement of a long bridge requires a big amount of measurement points, which extensively increases the involved measurement effort. Nonetheless, it could be used as control measurement with few measurement points at selected positions. The measurement with total station works automatically which decreased the measurement effort. The standard deviation of 0.2360 mm

presented in Figure 19 was reached without using reflector targets as the use of reflector targets decrease the measurement precision [43]. In contrast, the close-range photogrammetry based on high-quality cameras which were calibrated in advance and by using one of them on a drone provided an optimal application for bridge deflection measurement. The achieved accuracy for the full-frame camera D800 amounts to 0.1451 mm and for the medium format camera installed on the drone amounts to 0.1186 mm. The precision of the photogrammetry was not influenced by the vibration from the drone flight (Figure 18 A.). The zoom of the photogrammetric target number 11 is shown in Figure 18 A., which is captured while the drone flight. The low shutter speed of 1/500 sec and the robust gimbal of the drone allowed the avoidance of the camera shake effect. A very stable gimbal DJI Ronin-MX and a very short shutter speed of the camera could avoid the blurring effect. In comparison, a capture done from the tripod using the remote release is shown in Figure 18 B. In both pictures, the sharp and not blurred pixels from white to black are clearly visible. The image stabiliser from the lens was not used, which would otherwise negatively affect the measurement precision.

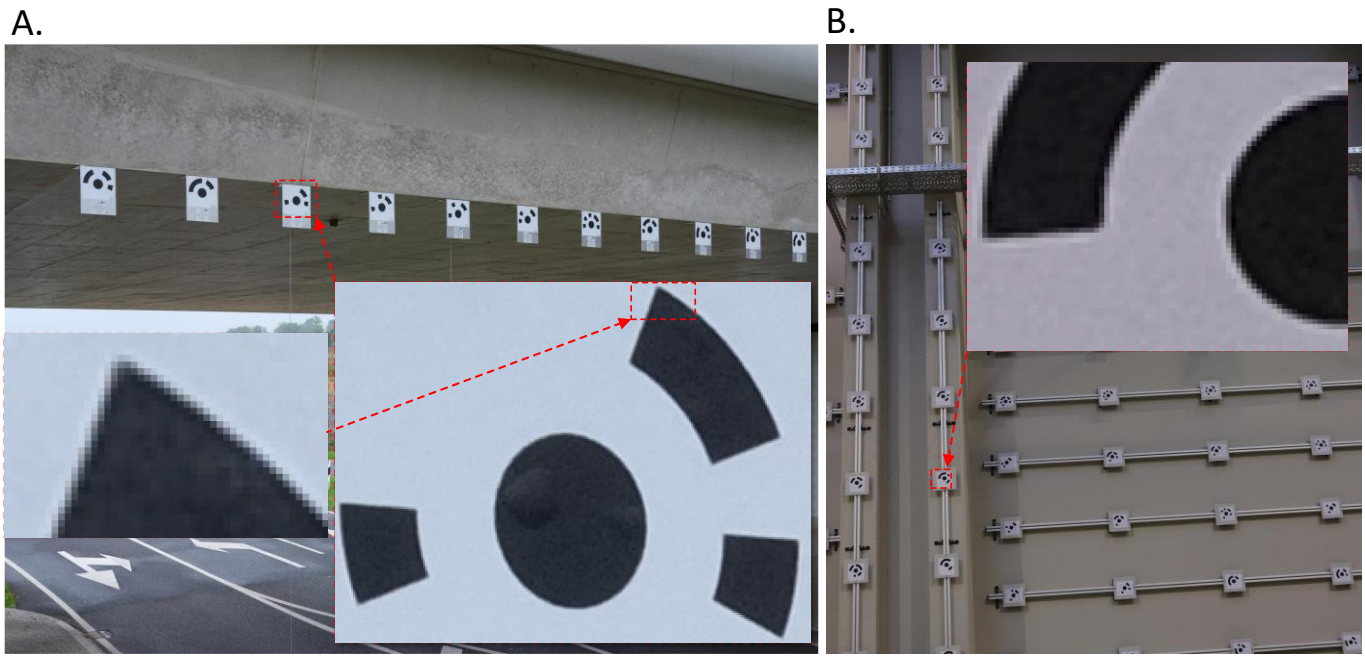

Figure 18. A. Capture while flying the drone without any blurring (shake) effect, B. capture done using tripod and remote release while calibration of the camera

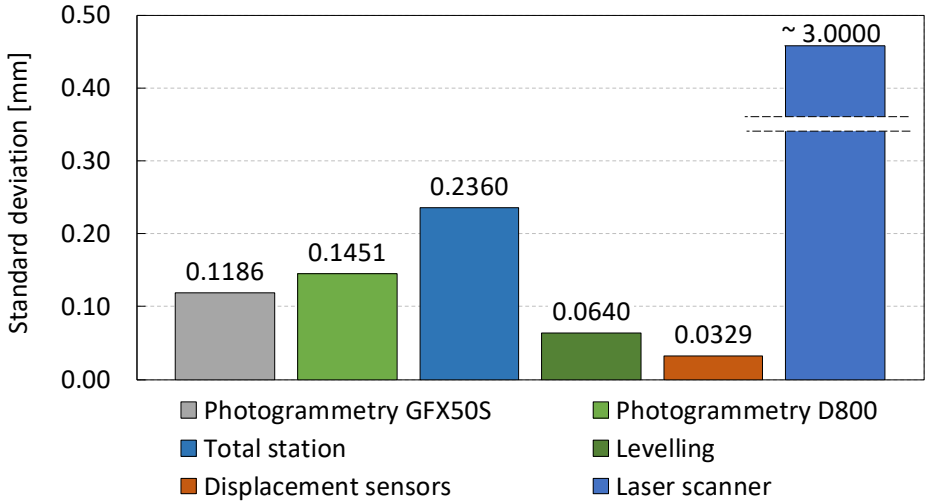

Figure 19. Reached precisions respectively standard deviations for the applied measurement techniques for deflection measurement

4.2. The damage detection and the DAD values

The detection of damage on the investigated bridge using the DAD method is carried out based on deflection measurements performed by photogrammetry and by levelling. The DAD values from photogrammetry is done for two different measuring point distances. The analysis and the background of the horizontal measuring point distance are published in [21]. The horizontal distance between the measuring points has a significant influence on the precision of damage detection. A closer range between the measuring points allows a higher precision on the localisation of the damage. However, the closer the measuring points, the smaller is the inclination angle change resulting from damage. However, the smaller the measurable inclination change, the higher is the required precision of the deflection measurement. Figure 20 and Figure 21 show the impact of the considered measuring point distance, namely 50 cm respectively 100 cm, on the calculation of DAD values based on photogrammetry.

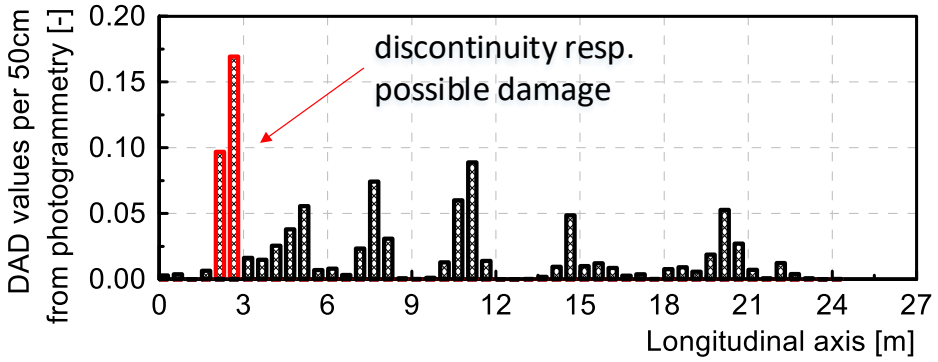

Figure 20. DAD values from curvature for measuring point distance of 50 cm and based on photogrammetry; red bars represent the outliers

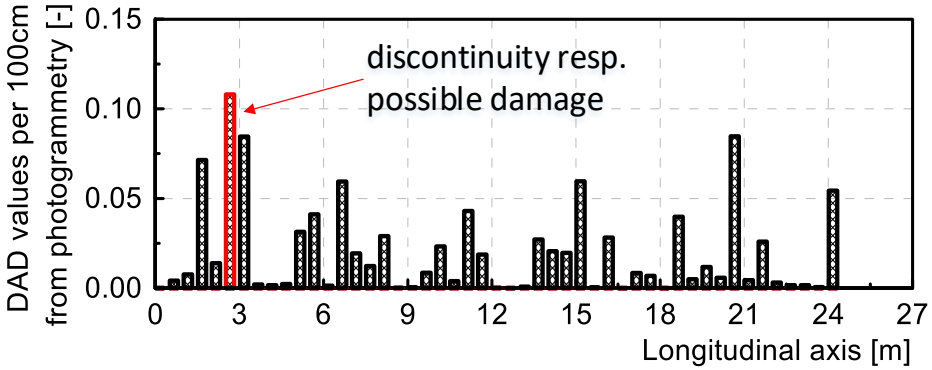

Figure 21. DAD values from curvature for measuring point distance of 100 cm and based on photogrammetry; red bars represent the outliers

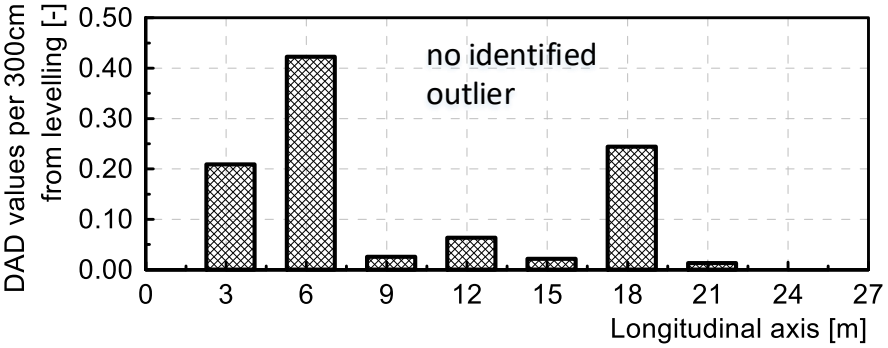

Figure 22. DAD values from curvature for measuring point distance of 300 cm and based on levelling

The outlier respectively the discontinuity of the DAD values were determined according to the method described in section 0. Figure 20 indicates some discontinuity at about 2.90 m. However, the discontinuity does not increase with increasing measurement point distance to 100 cm (Figure 21). As for smaller measuring point distances (Figure 20), the measurement noise has more influence on the DAD values than for bigger measuring point distances, the outlier in Figure 20 results from measurement noise and not from any damage. The DAD values for the measuring point distance of 100 cm present already a nearly uniform distribution so that it can be concluded that the structure is still undamaged. The results from photogrammetry in Figure 21 is confirmed by the accurate measurement with levelling, which also does not have any outlier as shown in Figure 22.

In summary, no damage was identified using the DAD method in the investigated bridge structure. However, the following questions require further clarification:

- Identifiable damage degree for bridge structures;
- Required precision of the measurement technique for localisation of small damages;

- Influence of damage position;
- Required maximum deflection;
- Number of required measurement repetition.

Therefore, an additional investigation is carried out to answer the questions as mentioned above. These investigations are based on FE calculations using a model with artificial noise effects to get realistic deflection measurement values, whereas the artificial noise introduced into the deflection line of the numerical model corresponds to the noise from the real measurements by photogrammetry for the bridge test.

5. Measurement noise and its influence

Theoretical examples showed that the DAD method is able to identify already smallest stiffness variations down to 1 % [20]. However, the detectability of the damage using the DAD method depends on several parameters. The most important factor is the precision of the deflection measurement. The close-range photogrammetry represented promising accuracy and application-oriented handling. Furthermore, the reached accuracy under laboratory condition was between 0.01 and 0.03 mm [40] [39] and for real bridge experiment between 0.10 and 0.14 mm. In the following sections, the influence of the measurement precision, the damage degree, the damage position, the required deflection size and the required number of measurement repetitions are investigated. The investigations are carried out based on a finite element model of the bridge Altrier from the experimental test.

5.1. Artificial noise

The calculation results from the finite element method deliver exact mathematical results without any noise effect. However, real measurements are always affected by normal-distributed noise effect. Therefore, realistic test results are generated from the finite element model by incorporating an artificial noise which is produced based on the measured standard deviation range from photogrammetry. The normal distributed pseudo-random number is generated using the function NORM.INV() from Microsoft Excel [44] based on the Wichmann and Hill theory [45]. The NORM.INV() function consists of the variables such as probability, standard deviation and the mean value as arguments. The probability is associated with the standard normal distribution (equation (10)).

$$f(x,\mu,\sigma) = \frac{1}{\sqrt{2\pi\sigma}} e^{-\left(\frac{(x-\mu)^2}{2\sigma^2}\right)} \tag{10}$$

The left diagram of Figure 23 shows the normally distributed noise effect for the standard deviation of 0.10 mm and the right diagram of Figure 23 illustrates the real measurement noise from photogrammetry. Both are not identical, but they have the same value of standard deviation and are distributed normally.

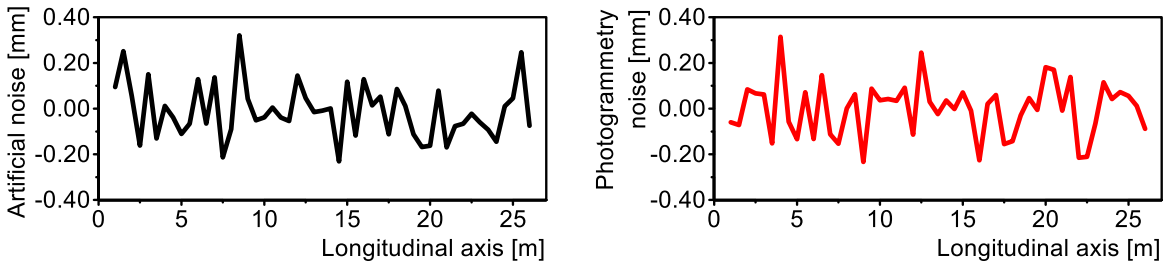

Figure 23. Left diagram: artificial noise, right diagram: real noise from photogrammetry measurement

5.2. Relation between the detectable degree of damage and the measurement precision for the use of DAD method

The detectable level of damage is investigated based on the measurement precision and the resulting DAD values. The study is done based on the theoretical model same to the static system of the experimental bridge. A local artificial damage is generated with several different levels by reducing the element stiffness. Figure 24 presents the DAD values from curvature at the damage position depending on the measurement precision and the damage level. The standard deviation varies from 0.01 mm to 0.10 mm. Each DAD value is determined from the average of 30 different calculations using artificial noise effects. A higher DAD value at a given damage position leads to more reliable damage identification. First, it can be considered that for smaller damage degrees, a higher precision of the deflection measurement is required. Furthermore, the trend lines of the relations between the precision of the measurement and the corresponding damage level follows an exponential curve.

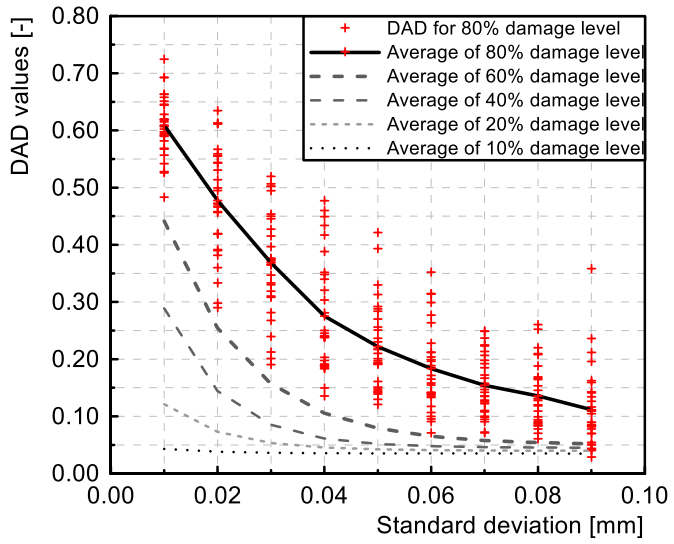

Figure 24. Relation between measurement precision and detectable degree of damage

5.3. Influence of the deflection size on the detectability of damage

Another significant factor influencing the damage detection using the DAD method is the size of the measured deflection. The maximum deflection of the bridge should not exceed a specific allowed value of deflection size not to exceed the serviceability limit state and to allow a non-destructive condition assessment. In principle, there is no clear regulation regarding the deflection limitation in bridge design standards. Nonetheless, there are indications for structural deflection limitation depending on the type of construction. The allowed size of deflection varies from L/350 to L/2000 [46] [47]. Figure 25 shows the analysis of the range of damage detection using the DAD method. The diagram illustrates nine different curves, which represent the DAD values for different experimental deflection sizes starting from L/600 to L/2500. The horizontal axis of the diagram shows the level of a local stiffness reduction due to damage. The two dashed lines in red and black indicate the detectability of damage in function of the measurement accuracy. The red dashed curve represents the detectability limit for a measurement accuracy of 0.09 mm, which corresponds to the accuracy of the photogrammetry of the real bridge experiment. The black dashed line illustrates the detectability limit corresponding to the accuracy of measurement at laboratory condition of 0.01 mm. All DAD values above the dashed boundary line point out successful identification of damage. For example, based on an experiment with maximal deflection of L/600, the reliable identifiable damage degree starts at 60 % for a measurement accuracy of 0.09 mm. With the measurement accuracy of 0.01 mm, the identification of damages at 30 % would be possible.

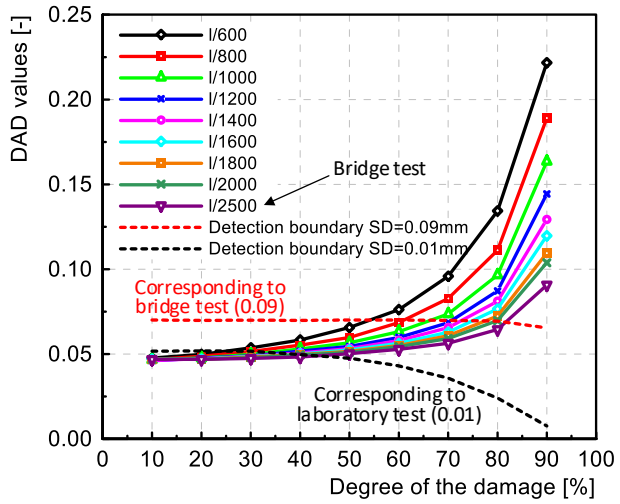

Figure 25. Damage identification based on deflection size and measurement precision

6. Influence of damage position on detection of damage

The position, at which damage has occurred, plays a role in the detection of damage using the DAD method. Figure 26 shows one-half of the studied FE-model. The influence of the damage position is examined on 30 measurements using random noise effects for each investigated position. The resulting DAD values are represented by an average line summarising the 30 measurements with the standard deviation of 0.03 mm indicated by single crosses in Figure 26 A. Figure 26 B. represents the resulting average trend lines from investigations with different standard deviations of 0.01 mm to 0.09 mm. A higher DAD value at the damage position corresponds to a more accurate damage localisation. The resulting DAD values clearly show that a better damage detection can be achieved closer to the maximum deflection area. In contrast, at a position with hardly any deflection, e.g. at the support structures, almost no damage can be detected.

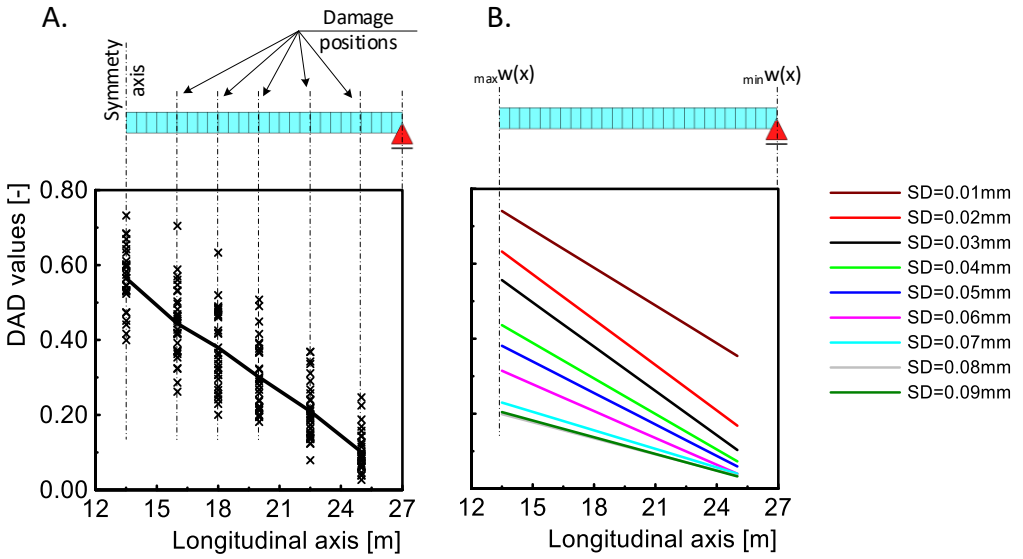

Figure 26. Influence of damage position on the detectability of damage

7. Influence of the repetition of measurements

The final investigation examines the influence of the repetition of the measurements on the variability of the resulting DAD values. This examination is carried out to understand how many deflection measurements are required to minimise the influence of measurement inaccuracy on the resulting DAD values. The problem is that the effect of normally distributed measurement noise involves potentially outliers, which could be falsely detected as damage. However, the repetition of the measurement would not have the potential outlier from measurement inaccuracy at the same area again. Only the outlier resulting from the damage would always highlight at the same position. Equation (11) is used to calculate the arithmetic mean values of the DAD values for n measurements. Mostly, the discontinuity resulting from damage effect is highlighted at the position of damage. However, some outliers resulting from the

measurement inaccuracy can occur randomly at various locations. The probability that an outlier resulting from noise effect occurs at the same location again is very low. Therefore, the repetition of the measurement helps to eliminate the effect of measurement noise and only to highlight discontinuities at the damage positions.

$$Average\ from\ n\ measurements = \frac{1}{n}\sum_{i=1}^{n} DAD_i(x) \tag{11}$$

Figure 27 shows the change of the DAD values at the damage position depending on the number of measurement repetitions. The presented DAD values cover the damage degrees from 10 % to 90 % and each value is based on average on ten artificially generated experimental values. The considered standard deviation amounts to 0.02 mm. The red curve illustrates the overall average from the nine different damage degrees. A stabilisation of the DAD values can be observed starting from the seventh repetition of the deflection measurements. In other words, the influence of the measurement noise effect can be optimally minimized starting from the seventh repetition of the measurements at a precision level of 0.02 mm. However, the number of required measurements varies depending on the measurement precision.

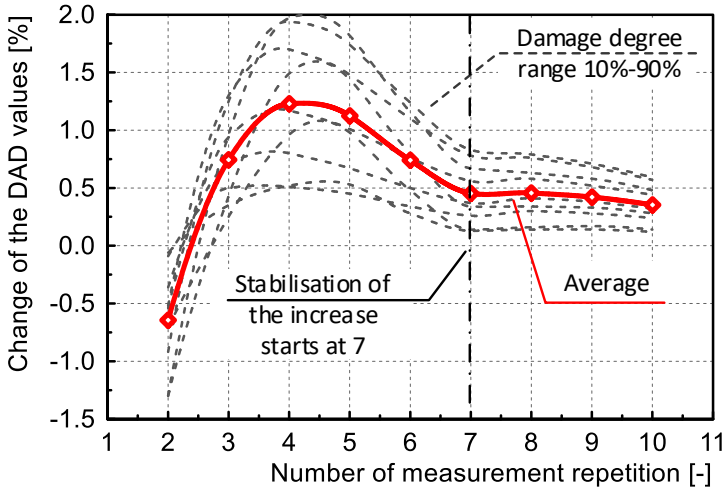

Figure 27. Influence of the measurement repetition on the precision of damage identification

8. Recommendation for practitioners

In principle, certain recommendations can be made for practitioners of the DAD method. With regard to the requirement for the measuring accuracy, it should be mentioned that the longer the span, the more precision is necessary. For multi-span bridges, it is advisable to position control points on every abutment. If the target can remain permanently on bridges, the exact location of the control points should be measured before each load-deflection experiment. The application of close-range photogrammetry with the help of a drone is highly recommended for larger, higher or even difficult accessible bridges. Nevertheless,

displacement sensors or levelling should be used as a control measurement. Concerning the experimental load, it is advisable to approach the serviceability limit state in order to produce a measurable deflection. It is recommended to repeat the measurements for statistical reasons, i.e. more than 7 times.

The used camera should be focused as far as possible on infinity. The shutter speed should be kept as short as possible to avoid blurring effect. The automatic rotation function of the camera and the image stabilizer of the lens must be switched off. Underexposed images are better than overexposed ones.

The measurement of the environment temperature, humidity or thermography is not required. The investigation of the measurement noise is not necessary, but the sensitivity of the DAD method would increase, if the measured deflection line is smoothed within the range of the standard deviation. The density of the target can be chosen comparable to the presented study such as 50 cm, however depending on the length of the structure. The smaller the span the more density of the measuring targets are required.

9. Conclusion

The presented work summarises the experiences of the application of the so-called “Deformation Area Difference” (DAD) method on the detection of damage in existing real bridge structures. The applied method is based on the relationship between bending moment and curvature. The essential prerequisites of the method are a high precision measurement of the deflection line from a static load deflection test and a simplified linear finite element model of the bridge structure. The presented real-scale experiment is carried out on a prestressed concrete bridge structure in Luxembourg with a span of 27 m. The applicability of the DAD method is investigated based on several modern measurement techniques, namely laser scanning, total station, levelling as well as displacement sensors and photogrammetry. The photogrammetry is applied on using a camera with a tripod taking pictures from multiple locations, and another camera on a drone, also taking pictures from various locations. The study deals with the precision of the measuring techniques and not with the accuracy. The accuracy gives an absolute value to a reference value, while the precision is a relative measurement value. The DAD method examines the measured deflection line relative to the reference curve. For the application of the DAD method a high precision measurement is sufficient.

From the findings of the different investigations, the following conclusions can be drawn:

- The reached precisions from the deflection measurements on the bridge structure amount to 0.1186 mm for photogrammetry, 0.236 mm for total station, 0.064 mm for levelling and 0.0329 mm for displacement sensors. As expected, no damage was detected on the newly constructed bridge structure using the DAD results from photogrammetry and levelling, which showed uniformly distributed values over the whole structure.

- Realistic experimental deflection measurement data was successfully generated based on theoretical models, which considered the artificial measurement noise effects.
- Theoretical models without measurement noise effect prove that the DAD method is able to detect smallest stiffness changes such as 1 % local damage.
- The influence of measurement precision is investigated based on finite element calculations with artificial measurement noise effect. The results showed that the effect of noise on lower measurement precision has an exponential influence on the damage detection.
- The size of the investigated structural deflection also has an essential impact, namely the higher the deflection, the lower is the damage level which can be detected.
- Damage close to higher deflections can be better localised than damage near to the support structures.
- The number of the measurement repetition is investigated to eliminate the falsely detected outliers resulting from measurement noise. The repetition number of more than seven delivered reliable interpretation about damage detection.

The applicability of the DAD method was already proven based on theoretical examples and laboratory tests [20] [21]. This study confirms the applicability of the DAD method on a real prestressed concrete bridge structure using most modern measurement techniques, especially with photogrammetry using a camera mounted on a big size drone delivered very promising results. Considering the discussed boundary conditions of the DAD method, this method offers a simple and reliable application for damage detection of bridge structures and contributes to the state-of-the-art of methods for condition assessment.

10. Acknowledgements

The authors would like to express their gratitude to the "Administration des Ponts et Chaussées" of Luxembourg for providing the opportunity to carry out experiments on a real bridge. Further gratitude is expressed to the team of Prof. Holger Voos of the University of Luxembourg for enabling the autonomous flight with the drone. Finally, special acknowledgements are expressed to the technical support team of the University of Luxembourg for their expertise and helpful contributions to the realisation of the large scale experiment.

References

[1] M. Pregnolato, "Bridge safety is not for granted - A novel approach to bridge management," *Engineering Structures,* vol. 196, pp. 109-193, 2019.

[2] Z. Kala, "Global sensitivity analysis of reliability of structural bridge system," *Engineering structures,* vol. 194, pp. 36-45, 2019.

[3] Y. Bao, Z. Chen, S. Wei, Y. Xu, Z. Tang and H. Li, "The State of the Art of Data Science and Engineering in Structural Health Monitoring," *Engineering,* vol. 5, pp. 234-242, 2019.

[4] S.-H. Huang, Y.-H. Huan, C. A. Blazquez and G. Paredes-Belmar, "Application of the an colony optimization in the resolution of the bridge inspection routing problem," *Applied Soft Computing,* vol. 65, pp. 443-461, 2018.

[5] W. Megid, M.-A. Chainey, P. Lebrun and R. Hay, "Monitoring fatigue cracks on eyebars of steel bridges using acoustic emission: A case study," *Engineering Fracture Mechanics,* vol. 211, pp. 198-208, 2019.

[6] E. A. Oskoui, T. Taylor and F. Ansari, "Method and monitoring approach for distributed detection of damage inmulti-span continuous bridges," *Engineering Structures,* vol. 189, pp. 385-395, 2019.

[7] B. Wu, G. Wu and C. Yang, "Parametric study of a rapid bridge assessment method usingdistributed macro-strain influence envelope line," *Mechanical Systems and Signal Processing,* vol. 120, pp. 642-663, 2019.

[8] M. M. Alamdari, K. Kildashti, B. Samali and H. V. Goudarzi, "Damage diagnosis in bridge structures using rotation influence line:Validation on a cable-stayed bridge," *Engineering Structures,* vol. 185, pp. 1-14, 2019.

[9] S.-Z. Chen, G. Wu and D.-C. Feng, "Damage detection of highway bridges based on long-gaugestrain response under stochastic traffic flow," *Mechanical Systems and Signal Processing,* vol. 127, pp. 551-572, 2019.

[10] J. Zhang, S. Guo, Z. Wu and Q. Zhang, "Structural identification and damage detection through long-gaugestrain measurements," *Engineering Structures,* vol. 99, pp. 173-183, 2015.

[11] B. Wu, G. Wu, C. Yang and Y. . He, "Damage identification method for continuous girder bridgesbased on spatially-distributed long-gauge strain sensing undermoving loads," *Mechanical Systems and Signal Processing,* vol. 104, pp. 415-435, 2018.

[12] N.-B. Wang, L.-X. He, W.-X. Ren and T.-L. Huang, "Extraction of influence line through a fitting method from bridgedynamic response induced by a passing vehicle," *Engineering Structures,* vol. 151, pp. 648-664, 2017.

[13] W.-J. Cao, C. G. Koh and I. Smith, "Contents lists available atScienceDirectEngineering Structuresjournal homepage:www.elsevier.com/locate/engstructEnhancing static-load-test identification of bridges using dynamic data," *Engineering Structures,* vol. 186, pp. 410-420, 2019.

[14] R. Jiang and D. V. Jauregui, "Development of a digital close-range photogrammetric bridge deflection measurement system," *Measurement,* vol. 43, pp. 1431-1438, 2010.

[15] P. J. Sousa, F. Barros, P. J. Tavares and P. M. Moreira, "Experimental measurement of bridge deflection using Digital Image Correlation," *Procedia Structural Integrity,* vol. 17, pp. 806-811, 2019.

[16] N. Le, D. Thambiratnam, A. Nguyen and T. Chan, “A new method for locating and quantifying damage in beams from staticdeflection changes,” *Engineering Structures,* vol. 180, pp. 779-792, 2019.

[17] M. Gatti, “Structural health monitoring of an operational bridge: A case study,” *Engineering Structures,* vol. 195, pp. 200-209, 2019.

[18] O. Mirza, S. K. Shill and J. Johnston, “Performance of Precast Prestressed Steel-Concrete Composite Panels Under Static Loadings to Replace the Timber Transoms for Railway Bridge,” *Structures,* vol. 19, pp. 30-40, 2019.

[19] E. O. Lantsoght, C. v. d. Veen, A. d. Boer and D. A. Hordijk, “State-of-the-art on load testing of concrete bridges,” *Engineering Structures,* vol. 150, pp. 231-241, 2017.

[20] D. Erdenebat, D. Waldmann, F. Scherbaum and F. N. Teferle, “The Deformation Area Difference (DAD) method for condition assessment of reinforced structures,” *Engineering Structures,* vol. 155, pp. 315-329, 2018.

[21] D. Erdenebat, D. Waldmann and N. Teferle, “Curvature based DAD-method for damage localisation under consideration of measurement noise minimisation,” *Engineering Structures,* vol. 181, pp. 293-309, 2019.

[22] X. Min and L. O. Santos, “Dynamic Assessment of the Sao Joao Bridge Structural Integrity,” *Procedia Structural Integrity,* vol. 5, pp. 325-331, 2017.

[23] S. Ataei and A. Miri, “Investigating dynamic amplification factor of railway masonry arch bridges through dynamic load tests,” *Construction and Building Materials,* vol. 183, pp. 693-705, 2018.

[24] H. Wang, J.-X. Mao and B. Spencer Jr, “A monitoring-based approach for evaluating dynamic responses of riding vehicle on long-span bridge unter strong winds,” *Engineering Structures,* vol. 189, pp. 35-47, 2019.

[25] M. d. Pristo, M. Scola and G. Zani, “On site assessment of Azzone Visconti bridge in Lecco: Limits and reliability of current techniques,” *Construction and Building Materials,* vol. 209, pp. 269-282, 2019.

[26] A. Bayraktar, T. Türker, J. Tadla, A. Kursun and A. Erdis, “Static and dynamic field load testing of the long span Nissibi cable-stayed bridge,” *Soil Dynamics and Earthquake Engineering,* vol. 94, pp. 136-157, 2017.

[27] N. Kovacs, B. Kövesdi, L. Dunai and B. Takacs, “Loading test of the Rákóczi bridge in Budapest,” *Procedia Engineering,* vol. 156, pp. 191-198, 2016.

[28] S. Maas, A. Zürbes, D. Waldmann, M. Waltering, V. Bungard and D. G. Roeck, “Damage assessment of concrete structures through dynamic testing methods. Part 2: Bridge tests,” *Engineering Structures,* vol. 34, pp. 483-494, 2012.

[29] V. H. Nguyen, S. Schommer, S. Maas and A. Zürbes, “Static load testing with temperature compensation for structural health monitoring of bridges,” *Engineering Structures,* vol. 127, pp. 700-718, 2016.

[30] A. Bakker, R. Biehler and C. Konold, “Should Young Students Learn about Box Plots?,” in *Curricular Development in Statistics Education*, Schweden, 2004.

[31] S. Lem, P. Onghena, L. Verschaffel and W. V. Dooren, “The heuristic interpretation of box plots,” *Learning and Instuction*, vol. 26, pp. 22-35, 2013.

[32] E. Standard, “EN 206-1,” CEN, Brussels, 2000.

[33] L. Geosystems, “Leica ScanStation P20,” Heerbrugg, Switzerland, 2013.

[34] L. Geosystems, “Leica TS30,” Heerbrugg, Switzerland, 2009.

[35] L. Geosystems, “Leica DNA Digitalnivelliere,” Heerbrug, Switzerland, 2006.

[36] “www.elcovision.com,” PMS Photo Mess Systeme AG, [Online]. Available: https://www.elcovision.com/d_pmsag_kontakt.html. [Accessed 26 08 2019].

[37] “www.hbm.com,” Höttinger Baldwin Messtechnik GmbH. [Online]. [Accessed 26 08 2019].

[38] “http://vbi.truck.volvo.com/index.php,” 23 August 2019. [Online]. Available: http://vbi.truck.volvo.com/index.php.

[39] D. Erdenebat, D. Waldmann and F. N. Teferle, “Static load deflection experiment on a beam for damage detection using the Deformation Area Difference Method,” in *IALCCE*, Ghent, 2018.

[40] D. Erdenebat, D. Waldmann and F. N. Teferle, “Laboratory experiment for damage assessment using the DAD-method,” in *SMAR*, Zurich, 2017.

[41] D. Erdenebat and D. Waldmann, “Condition assessmend and damage localisation for bridges by use of Deformation Area Difference Method (DAD-Method),” in *fib Symposium*, Cape Town, 2016.

[42] G. f. G. G. u. L. DVW, “Terrestrisches Laserscanning 2018,” Wißner-Verlag, Augsburg, 2018.

[43] “Berntsen,” 05 11 2013. [Online]. Available: https://berntseninternational.com/Home/News-Events/ArtMID/1869/ArticleID/16/Understanding-the-Differences-Between-Reflective-Targets-and-Prism-Survey-Systems. [Accessed 10 10 2019].

[44] E. Jeschke, H. Reinke, S. Unverhau, E. Pfeifer, B. Fienitz and J. Bock, Excel 2010 Formulas & Functions Inside Out, Washington: Microsoft Press, 2012.

[45] B. Wichmann and I. Hill, “Generating good pseudo-random numbers,” *Computational Statistics & Data Analysis*, vol. 51, pp. 1614-1622, 2006.

[46] N. N. M. Kyaw, K. L. Htat and S. Y. Khaing, “Investigation on the Behaviours of Long-Span Suspension Bridge with Self Anchorage System,” *International Journal of Science, Engineering and Technology Research*, vol. 3, no. 6, pp. 1697-1700, 2014.

[47] F. Samim and S. Nakamura, “Study on Serviceability of Cable-Stayed Bridges,” *Proceedings of the School of Engineering of Tokai University*, vol. 40, pp. 21-28, 2015.

639

640